INTEGRATION OF HYDROGEL ADHESIVE AND MICROSTRUCTURED DEVICE FOR VAGUS NERVE STIMULATION

Jae Young Park[1,2,3], Jongcheon Lim[1,2,3*], Carl R. Russell III[1], Pei-Lun Chen[1], Seokkyoon Hong[1], Chi Hwan Lee[1], and Hyowon Lee[1,2,3†]*

[1]Weldon School of Biomedical Engineering, Purdue University, West Lafayette, IN, USA
[2]Birck Nanotechnology Center, Purdue University, West Lafayette, IN, USA
[3]Center for Implantable Devices, Purdue University, West Lafayette, IN, USA

ABSTRACT

Vagus nerve stimulation (VNS) is an established therapeutic intervention for a range of neurological conditions.[1] However, conventional VNS methodologies are hindered by challenges such as high-pressure distribution, intricate cuffing techniques, and the maintenance of consistent electrode contact. In this research, we have developed an advanced cervical VNS platform that integrates ultra-thin (~3μm) microstructured electrodes with a hydrogel adhesive. This innovative design ensures consistent contact with the vagus nerve, effectively minimizing electrode migration, which is fatal to consistent therapeutic efficacy[2]. Upon application, the hydrogel adhesive forms a uniformly cross-linked interface with primary amine groups on the nerve, utilizing the void space in the kirigami pattern to secure the thin-film electronic device in place. The hydrogel adhesive is composed of a non-adhesive, hydrophilic polyurethane (PU) top layer and a bioadhesive bottom layer. The synergistic combination of a microstructured thin-film device and adhesive polymer exhibits significant promise for a biocompatible, suture-less, soft and stable VNS cuff.

KEYWORDS

Vagus nerve stimulation, Hydrogel adhesive, stretchable, microfabrication

INTRODUCTION

Vagus nerve stimulation (VNS) has been recognized as an effective therapy for treating neurological conditions like drug-resistant epilepsy[1] and depression[3]. The procedure involves implanting a neural electrode on the cervical vagus nerve to deliver electric charges that activate nerve, achieving therapeutic benefits. Traditional cuff electrodes, made from a helix of silicone rubber (~0.5 mm thick, 2MPa) and platinum (~2.5 μm thick, ~200GPa), exhibit a significant mismatch in mechanical properties and shape compared to neural tissue (~100kPa)[4], potentially causing a foreign body reaction and leading to device encapsulation by scar tissue.[5], [6]

To overcome these issues, thin-film material with smaller volumes like polyimide and perylene-c have been suggested. [7], [8], [9], [10] Nevertheless, the stiffness (~2GPa) still causes challenges.[11] Recent advancements are aimed at improving ttthe stretchability, by utilizing microstructured patterns like serpentine on thin film substrates or soft elastomers [12], [13]

Stable contact between the electrode and nerve is essential for efficient stimulation, as poor contact increase interfacial impedance and reduce stimulation effectiveness. [2] The needs for precise stimulation even more critical when targeting specific nerve fibers to minimize off-target effects, requiring stable electrode placement without shifting. [14], [15], [16]. While applying pressure around the nerve could potentially harm the internal fibers, it's important to exert some pressure to maintain a stable connection between the electrode and the nerve. [17]

In response, our study introduces a cutting-edge VNS cuff that combines ultrathin Y-shaped kirigami electrodes with a hydrogel adhesive, as illustrated in Fig 1a. This design not only ensures stable nerve contact, minimizing electrode movement but also facilitates targeted activation of c-fibers. The hydrogel adhesive creates a secure connection with covalent bonds between the nerve and the electrode, eliminating the need for sutures and reducing the pressure applied to the nerve. The device's adaptability to nerve geometry changes is enhanced by the swellable nature of the hydrogel adhesive upon hydration, which becomes highly compliant. As illustrated in Fig 1b, this, along with the kirigami void pattern, allows for uniform contact across the electrode surface. Our innovative approach promises a biocompatible, non-suturing, flexible, and stable solution for VNS therapy.

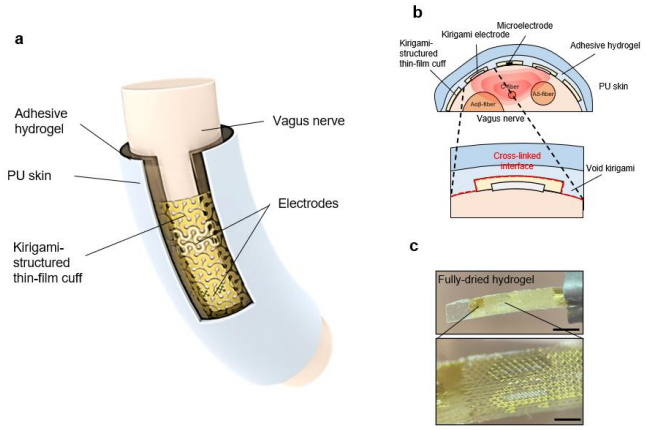

Figure 1 (a) Schematic illustration of hydrogel-kirigami device implanted on vagus nerve. (b) cross section of the implanted interface. (c) photographs of the device in dry state. Scale bar = 3 mm (up) and 1 mm (down).

MATERIALS AND METHODS

Device Fabrication

The polyimide resin (PI 2545, HD Microsystems, Parlin, NJ) was applied to 100-mm silicon wafer through spin-coating (thickness = 1.5 μm) and baked at 300 °C. To create the pattern for metal trace, we utilized a positive photoresist (PR, AZ9260, MicroChem, Newton, MA, USA). A maskless aligner (MLA150, Heidelberg Instruments, Germany) was used for photolithography. After the 1st photolithography, 10 nm of titanium (Ti) and 100 nm of platinum (Pt) was sputtered and followed by a lift-off process. Top PI layer, serving as a passivation layer (thickness = 1.5 μm) is patterned using the reactive ion etch (RIE) with oxygen plasma (O_2 at 50 sccm, 100W, 50 mTorr for 60 min) to define the outline. This is done through a 20 μm thick photoresist barrier, applied through a double-spinning and then patterned. The sample procedure was applied for opening for the stimulating electrodes. After optical inspection, the devices were released from the silicon substrate with buttered oxide etch (BOE) and rinsed with deionized water.

978-1-940470-05-4/HH2024/$25©2024TRF
DOI 10.31438/TRF.HH2024.83

PVA-PAA-NHS ester-based hydrogel adhesive fabrication

The hydrogel adhesive with PVA-PAA-NHS ester was prepared following the methodology outlined by Wu et al. (2022)[18]. The preparation of the precursor solution involves specific material ratio: 35% (w/w) acrylic acid (AAc, Cat. No. 147230, Sigma-Aldrich, St-Louis, MO, USA), 0.2% (v/v) α-ketoglutaric acid (Cat. No. K1128, Sigma-Aldrich, St-Louis, MO, USA), 0.05% (w/w) poly(ethylene glycol) dimethacrylate (PEGDMA, Cat. No. 409515, Sigma-Aldrich, St-Louis, MO, USA), 7% (w/w) poly(vinyl alcohol) (PVA, Cat. No. 363065, Sigma-Aldrich, St-Louis, MO, USA) in DI water. To produce 100ml of this solution, 58 ml of DI water is was heated and stirred with 7g PVA at 140˚C at 300rpm overnight. After cooling to RT at a reduced stirring speed of 50rpm, 35ml of AAc, 50µl of polyethylene glycol dimethacrylate (PEGDMA), and 0.2g of α-ketoglutaric acid were added and left under RT overnight. Just prior to curing, 10 mg of acrylic acid *N*-succinimidyl ester (AAc-NHS ester, Cat. No. 409510, Thermo Fisher Scientific, Waltham, MA, USA) per 1ml of precursor solution was thoroughly mixed through syringe.

For the curing process, molds was prepared using water-repellent glass slides and Kapton® tape (~ 30µm) (Creative Global Services, Inc., USA) as spacers. The mixed solution was dispensed on the glass, covered with another slide, and then cured under UV light (wavelength 365 nm) for 30 min. After curing, the top slide was gently removed, and the hydrogel film was stored in a nitrogen-purged chamber.

Amine functionalization on PI

To establish a robust chemical crosslink between PI and the hydrogel, the PI surface was functionalized with a primary amine group using a method previously described.[11]. Initially, the PI was cleaned using IPA, DI, and O_2 plasma treatment for 3 min (30 W, 150 sccm). After the cleaning, to form primary amine groups on the PI surface, the film was immersed in 10% (w/v) hexamethylenediamine (HMDA, Sigma-Aldrich, Cat. No. H11696) aqueous solution for 24 hours in room temperature. After incubation. The PI substrates were thoroughly rinsed with DI water and dried with N_2 flow.

Surgical procedures

All procedures involving animals were conducted with the approval of the Purdue Animal Care and Use Committee (PACUC) under approval number 1112000390. The procedure began with a midline incision from the midpoint of the caudal ends of the mandibles extending to the manubrium of the sternum. Through blunt dissection, connective tissues were cleared until the left cervical vagus nerve was visible and distinctly isolated from the surrounding connective tissue.

RESULTS AND DISCUSSION

Mechanical properties of kirigami-structured trace and hydrogel

To verify the stretchability, tensile test and electromechanical test was conducted as illustrated in Fig 2a. In both dried hydrogel and PU/hydrogel composite, the Young's modulus surpasses 140MPa, yet it significantly softens to below 100 kPa once hydrated (Fig 2b). This softening renders the modulus not only much lower than both silicone-based cuff (~ 2MPa) and nerves (~100kPa), while being similar to the consistency of brain tissue. Such a property allows for the manipulation of thin-film Kirigami configurations as if they were rigid backbones, which then becomes pliable when applied to moist tissue. Adding hydrophilic polyurethane (PU) to the adhesive composition of the hydrogel changes its mechanical characteristics. The Young's modulus decreases slightly in the dried form of the hydrogel but rises in the presence of moisture, positioning the modulus of hydrophilic PU between the dry and hydrated states of the hydrogel.

In addition, bare thin-film and two variations of kirigami-patterned traces showed distinct electrical behaviors under stress as shown in Fig 2c. The kirigami designs, labeled R40 and R20, were remarkably less sensitive to strain, retaining their connectivity well past 30% elongation, which surpasses the swelling ratio previously noted in healthy nerve group (12-14%, ulnar nerve)[19], whereas the bare trace lost integrity at just below 3.5% elongation. These findings underscore the kirigami design's ability to sustain reliable electrical connections under the variable conditions of physiological environments.

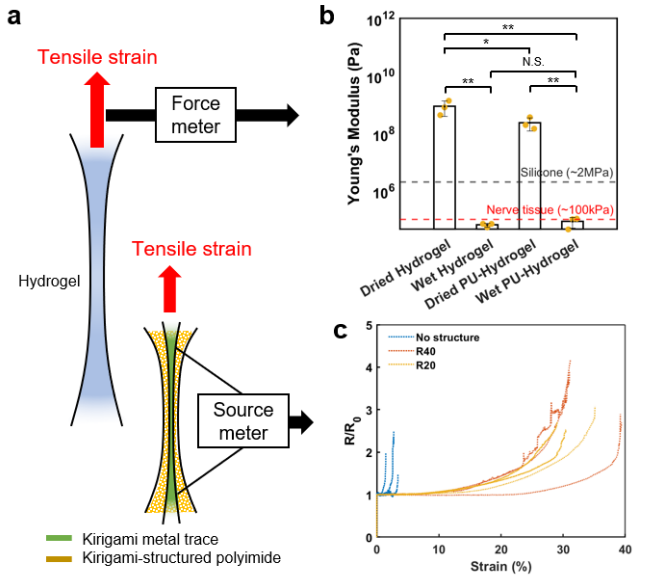

Figure 2 (a) Schematic illustration of stretchability tests. (b) Young's modulus of hydrogel adhesive and PU/hydrogel adhesive in dry and wet state. (c) Electromechanical test of kirigami trace.

Adhesion test for tissue/hydrogel adhesive/PI interface

The study also examined how well biological tissue sticks to the hydrogel over time when pressed lightly, to mimic actual implant conditions and determine the best incubation period as shown in Fig 3a. Additionally, one side was secured with a fully incubated, functionalized PI/hydrogel coating because the weakest link tends to fail mechanically, and the bond strength of the functionalized PI/hydrogel after overnight incubation was much stronger than that between porcine tissue and hydrogel. According to Fig 3b, the bonding strength between porcine skin and PI grew with incubation time and was significantly better than that of the non-crosslinked group, which lacked crosslinkers (AAc-NHS ester). The bond's toughness after 1 minute was comparable to, or better than, that of existing commercial tissue adhesives, indicating that quick application of the hydrogel-kirigami cuff is feasible.

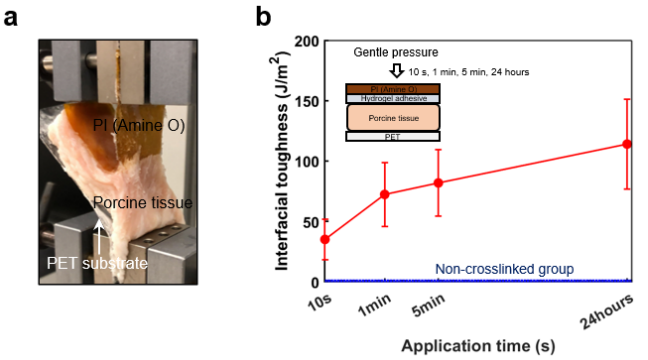

Figure 3 (a) Photograph of T-peel test between porcine tissue and amine functionalized PI crosslinked through hydrogel adhesive. (b) interfacial toughness according to the incubation time.

Contact stability test

The stability of electrode contacts within the device, featuring an amine-functionalized interface where the hydrogel adhesive is evenly crosslinked across the void sapces in kirigami trace, was evaluated as shown in Fig 4a. This process involved attaching a bilayer of the device/PI film to two glass slides, submerging them in 1x PBS for 10 minutes to remove any dried adhesion at the interface, and then exerting shear strain on the top glass while the bottom was held stationary with a custom jig. Groove lines, laser-engraved periodically on the PI film, served to track shifts in the microelectrodes train. Shear stress was applied to the sample by increasing the gap between the two glasses to 5 mm, followed by stress relief by returning the gap to 0. The interface with crosslinked adhesive demonstrated a notably smaller shift in electrode position compared to the non-crosslinked group. Quantitative analysis revealed that this difference became significant at displacements over 2 mm, suggesting that shear stress beyond this point surpasses the adhesive strength of the non-crosslinked interface, whereas it remains below the threshold for the crosslinked interface. (Fig 4b) Furthermore, electrodes at the crosslinked interface realigned to their original positions once the stress was removed, unlike those in the non-crosslinked group, which exhivited substantial shifts. (Fig 4c) This indicates that electrode movement in the crosslinked interface is primarily due to hydrogel deformation under shear stress, with positions recovering as the deformation subsides. These findings underscore the enhanced stability and resilience of the crosslinked hydrogel in preserving electrode placement.

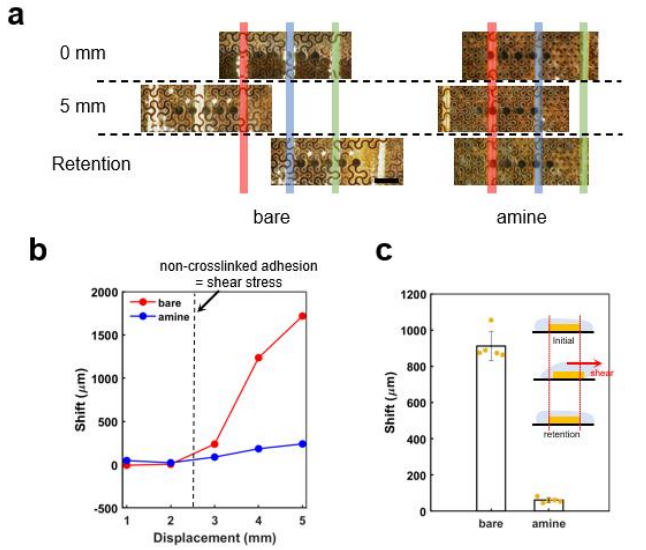

Figure 4 (a) electrode stability test results under shear stress. The results were quantified in (b) and (c).

Summary and Future Plan

In this research, a novel, sutureless, highly-compliant, stable interface for VNS was developed by combining a hydrogel adhesive and a microfabricated device through crosslinking process. The stretchability, strong adhesion, and high contact stability were verified through multiple benchtop studies. In vivo validation will follow to demonstrate the functionality.

REFERENCES

[1] D. H. Toffa, L. Touma, T. El Meskine, A. Bouthillier, and D. K. Nguyen, "Learnings from 30 years of reported efficacy and safety of vagus nerve stimulation (VNS) for epilepsy treatment: A critical review," *Seizure*, vol. 83, pp. 104–123, Dec. 2020, doi: 10.1016/j.seizure.2020.09.027.

[2] D. T. Brocker and W. M. Grill, "Principles of electrical stimulation of neural tissue," 2013, pp. 3–18. doi: 10.1016/B978-0-444-53497-2.00001-2.

[3] S. E. Krahl, S. S. Senanayake, A. E. Pekary, and A. Sattin, "Vagus nerve stimulation (VNS) is effective in a rat model of antidepressant action," *J Psychiatr Res*, vol. 38, no. 3, pp. 237–240, May 2004, doi: 10.1016/j.jpsychires.2003.11.005.

[4] G. H. Borschel, K. F. Kia, W. M. Kuzon, and R. G. Dennis, "Mechanical properties of acellular peripheral nerve," *Journal of Surgical Research*, vol. 114, no. 2, pp. 133–139, Oct. 2003, doi: 10.1016/S0022-4804(03)00255-5.

[5] G. G. Naples, J. T. Mortimer, A. Scheiner, and J. D. Sweeney, "A spiral nerve cuff electrode for peripheral nerve stimulation," *IEEE Trans Biomed Eng*, vol. 35, no. 11, pp. 905–916, 1988, doi: 10.1109/10.8670.

[6] W. B. Tarver, R. E. George, S. E. Maschino, L. K. Holder, and J. F. Wernicke, "Clinical Experience with a Helical Bipolar Stimulating Lead," *Pacing and Clinical Electrophysiology*, vol. 15, no. 10, pp. 1545–1556, Oct. 1992, doi: 10.1111/j.1540-8159.1992.tb02933.x.

[7] Z. Xiang *et al.*, "Progress of Flexible Electronics in Neural Interfacing – A Self-Adaptive Non-Invasive Neural Ribbon Electrode for Small Nerves Recording,"

Advanced Materials, vol. 28, no. 22, pp. 4472–4479, Jun. 2016, doi: 10.1002/adma.201503423.
[8] S. Lee *et al.*, "Selective stimulation and neural recording on peripheral nerves using flexible split ring electrodes," *Sens Actuators B Chem*, vol. 242, pp. 1165–1170, Apr. 2017, doi: 10.1016/j.snb.2016.09.127.
[9] N. Xue *et al.*, "Polymeric C-shaped cuff electrode for recording of peripheral nerve signal," *Sens Actuators B Chem*, vol. 210, pp. 640–648, Apr. 2015, doi: 10.1016/j.snb.2015.01.006.
[10] D. N. Heo *et al.*, "Flexible and Highly Biocompatible Nanofiber-Based Electrodes for Neural Surface Interfacing," *ACS Nano*, vol. 11, no. 3, pp. 2961–2971, Mar. 2017, doi: 10.1021/acsnano.6b08390.
[11] D. J. Tyler and D. M. Durand, "Chronic Response of the Rat Sciatic Nerve to the Flat Interface Nerve Electrode," *Ann Biomed Eng*, vol. 31, no. 6, pp. 633–642, Jun. 2003, doi: 10.1114/1.1569263.
[12] B. Ji *et al.*, "Stretchable Parylene-C electrodes enabled by serpentine structures on arbitrary elastomers by silicone rubber adhesive," *Journal of Materiomics*, vol. 6, no. 2, pp. 330–338, Jun. 2020, doi: 10.1016/j.jmat.2019.11.006.
[13] Y. Zhang *et al.*, "Climbing-inspired twining electrodes using shape memory for peripheral nerve stimulation and recording," *Sci Adv*, vol. 5, no. 4, Apr. 2019, doi: 10.1126/sciadv.aaw1066.
[14] A. Fitchett, S. Mastitskaya, and K. Aristovich, "Selective Neuromodulation of the Vagus Nerve," *Front Neurosci*, vol. 15, May 2021, doi: 10.3389/fnins.2021.685872.
[15] S. L. Blanz *et al.*, "Spatially selective stimulation of the pig vagus nerve to modulate target effect versus side effect," *J Neural Eng*, vol. 20, no. 1, p. 016051, Feb. 2023, doi: 10.1088/1741-2552/acb3fd.
[16] N. Thompson *et al.*, "Fascicular Organisation and Neuroanatomy of the Porcine and Human Vagus Nerves: Allowing for Spatially Selective Vagus Nerve Stimulation," *The FASEB Journal*, vol. 36, no. S1, May 2022, doi: 10.1096/fasebj.2022.36.S1.R3366.
[17] D. J. Tyler and D. M. Durand, "Chronic Response of the Rat Sciatic Nerve to the Flat Interface Nerve Electrode," *Ann Biomed Eng*, vol. 31, no. 6, pp. 633–642, Jun. 2003, doi: 10.1114/1.1569263.
[18] J. Wu *et al.*, "An off-the-shelf bioadhesive patch for sutureless repair of gastrointestinal defects," *Sci Transl Med*, vol. 14, no. 630, Feb. 2022, doi: 10.1126/scitranslmed.abh2857.
[19] H. Letissier, G. Dardenne, A. Saraux, D. Le Nen, B. Borotikar, and S. Jousse-Joulin, "Correction to: Ultrasound Ulnar Nerve Measurement in a Healthy Population," *Rheumatol Ther*, vol. 8, no. 2, pp. 1049–1049, Jun. 2021, doi: 10.1007/s40744-021-00319-7.

CONTACT

*H. Lee, hwlee@purdue.edu